Progress In Electromagnetics Research, PIER 82, 137–150, 2008

INFLUENCE OF EXTERNAL MAGNETIC FIELD ON A SYMMETRICAL GYROTROPIC SLAB IN TERMS OF GOOS-HÄNCHEN SHIFTS

H. Huang † **and Y. Fan**

School of Electrical Engineering
Beijing Jiaotong University
Beijing 100044, P. R. China

F. Kong

School of Information Science and Engineering
Shandong University
Jinan 250100, P. R. China

B.-I. Wu and J. A. Kong

Research Laboratory of Electronics
Massachusetts Institute of Technology
Cambridge, MA02139, USA

Abstract—A detailed study on the influence of an external magnetic field on a symmetrical gyrotropic slab in terms of Goos-Hänchen (GH) phase shifts is presented. The GH phase shifts at both boundaries of the slab are calculated, and the guidance condition is explained by means of them. It is found that the external magnetic field destroys the spatial symmetry of the field distribution, and we use the concepts of 'penetration' distance as well as effective thickness to illustrate the phenomenon. In term of the GH phase shifts, the spatial distribution of the time-average Poynting power is also derived. We find that influenced by the external magnetic field, the positive and negative time-average Poynting power along the waveguide direction can exist simultaneously in the gyrotropic medium, depending on the transverse position.

† Also with Research Laboratory of Electronics, Massachusetts Institute of Technology, Cambridge, MA02139, USA

1. INTRODUCTION

The characteristics of the propagation of electromagnetic radiation in gyrotropic plasmas have been theoretically investigated in many literatures. The magnetoplasma modes in Voigt, perpendicular, and Faraday configurations have been studied by Kushwaha and Halevi [1–3]. Gillies and Hlawiczka have done some researches on gyrotropic waveguide in detail [4–8], and dyadic Green's functions for gyrotropic medium have been investigated by Eroglu as well as Li [9–11]. There are also some studies focusing upon the effects of magnetic field on semiconducting plasma slab [12], and on negatively refracting surfaces [13]. Furthermore, propagation and scattering characteristics in gyrotropic systems [14–19], surface modes at the interface of a special gyrotropic medium [20], applications of gyrotropic material to microwave technologies [21, 22], bilateral coplanar waveguides [23], finite layered structures [24–26], guided devices [27, 28], and manipulation of terahertz surface plasmons [29] have been investigated extensively. Moreover, Sarid mentioned that external magnetic field can destroy the spatial symmetry of the guided modes in a thin metal film [30].

In this paper, we will study the Goos-Hänchen (GH) phase shifts on both sides of the symmetrical gyrotropic slab, and derive the guidance condition. The distribution of the magnetic and electric fields for the waveguide modes and surface modes will be presented in terms of the GH phase shifts. Furthermore, to get deeper insight into the physics of such waves, we also calculate the time-average Poynting vector along the waveguide and show its spatial distribution. For the first time, we find that influenced by the external magnetic field, the positive and negative time-average Poynting power along the waveguide direction can exist simultaneously in the gyrotropic medium, depending on the transverse position.

2. GUIDED MODE DISPERSION LAWS

We consider a homogeneous infinite gyrotropic slab of thickness d in the Voigt configuration. i.e., the external magnetic field $\bar{B}_0$ is parallel to the interfaces and perpendicular to the wave propagating direction, as shown in Fig. 1. The media in region 1 and region 3 are the same and are isotropic, with permeability μ_1 and permittivity ε_1. Region 2 is gyrotropic medium with permeability μ_2 and permittivity tensor $\bar{\bar{\varepsilon}}_2$,

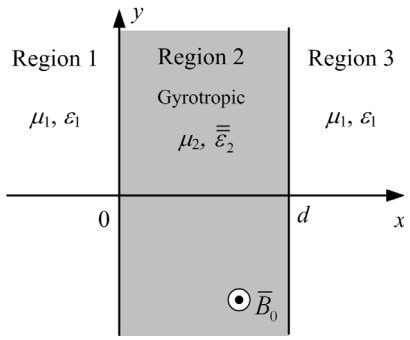

Figure 1. Symmetrical gyrotropic slab waveguide of thickness d in an isotropic medium. Region 1 and Region 3 are the same isotropic medium, with permittivity ε_1 and permeability μ_1. Region 2 is a gyrotropic medium. The wave propagates in y direction. And an applied magnetic field $\bar{B}_0$ is in the z direction, parallel to the interfaces and perpendicular to the wave propagating direction (Voigt configuration).

which takes the following form:

$$\overline{\overline{\varepsilon}}_2 = \begin{bmatrix} \varepsilon_{xx} & i\varepsilon_g & 0 \\ -i\varepsilon_g & \varepsilon_{yy} & 0 \\ 0 & 0 & \varepsilon_{zz} \end{bmatrix}, \tag{1}$$

where elements are given by

$$\varepsilon_{xx} = \varepsilon_{yy} = \varepsilon_\infty \left(1 - \frac{\omega_p^2}{\omega^2 - \omega_c^2}\right), \tag{2a}$$

$$\varepsilon_{zz} = \varepsilon_\infty \left(1 - \frac{\omega_p^2}{\omega^2}\right), \tag{2b}$$

$$\varepsilon_g = \varepsilon_\infty \left[-\frac{\omega_p^2 \omega_c}{\omega\left(\omega^2 - \omega_c^2\right)}\right]. \tag{2c}$$

Here, the off-diagonal element ε_g is a direct manifestation of the applied magnetic field. The quantities $\omega_p = \sqrt{Nq_e^2/(m^*\varepsilon_\infty)}$ and $\omega_c = q_e B_0/m^*$ are the plasma and cyclotron frequencies, corresponding to the characteristics of the medium and the external magnetic field respectively, ε_∞ is the background permittivity, N is the electron density, m^* is the effective mass, and q_e is the electron charge.

It is known that in the Voigt configuration, the TE mode is not coupled to the TM mode and only the TM mode is affected by the gyrotropy [12, 13]. Hence we only focus on the TM wave in this paper. For TM waves, with wave vectors $\pm\hat{x}k_x+\hat{y}k_y$ in the gyrotropic medium and $\pm\hat{x}i\alpha_1+\hat{y}k_y$ in the isotropic medium, the dispersion relations can be expressed as

$$k_y^2 + k_x^2 = \omega^2\mu_2\varepsilon_V, \tag{3}$$

$$k_y^2 - \alpha_1^2 = \omega^2\mu_1\varepsilon_1, \tag{4}$$

where k_y and k_x are wave numbers in gyrotropic medium in the y and x directions respectively, and α_1 is a positive real number that corresponds to the evanescent waves in the isotropic medium. Noting that k_x can be either purely real (corresponding to waveguide modes) or purely imaginary (corresponding to the surface modes decaying exponentially away from both interfaces), we assume k_x to be positive or with the positive imaginary part k_{xI}. And ε_V, defined as $\varepsilon_V = (\varepsilon_{xx}^2 - \varepsilon_g^2)/\varepsilon_{xx}$, is the equivalent permittivity of the gyrotropic medium in the Voigt configuration for the waves being studied.

To find the guidance condition, we consider the reflection coefficient when total reflection occurs on each side of the slab. Using the Maxwell equations and matching the boundary conditions, which enforce the tangential component of magnetic and electric fields to be continuous, we can get the reflection coefficients R_0 (corresponding to the boundary at $x = 0$) and R_d (corresponding to the boundary at $x = d$) at total reflection:

$$R_0 = \frac{1-i(p-q)}{1+i(p-q)} = e^{-i2\tan^{-1}(p-q)} = e^{i2\phi_0}, \tag{5}$$

$$R_d = \frac{1-i(p+q)}{1+i(p+q)}e^{i2k_xd} = e^{-i2\tan^{-1}(p+q)}e^{i2k_xd} = e^{i2\phi_d}e^{i2k_xd}, \tag{6}$$

where the phase shift $2\phi_0$ and $2\phi_d$ are the GH phase shifts at the two boundaries and can be expressed as

$$2\phi_0 = -2\tan^{-1}(p-q), \tag{7}$$

$$2\phi_d = -2\tan^{-1}(p+q), \tag{8}$$

where the parameters p and q are defined as

$$p = \frac{\varepsilon_V\alpha_1}{\varepsilon_1 k_x} \quad \text{and} \quad q = \frac{\varepsilon_g k_y}{\varepsilon_{xx}k_x}. \tag{9}$$

It is clear that, influenced by the applied magnetic field, these two shifts are not the same for guided wave components traveling in the

$+x$ and $-x$ directions. When there is no external magnetic field, i.e., $\varepsilon_g = 0$, and the parameter q in Eqs. (7) and (8) is zero, hence the GH phase shifts on both sides are the same. When the magnetic field is applied, the element ε_g in the permittivity tensor arises, making the medium nonreciprocal, and q is no longer zero, which results in the different GH phase shifts.

The guidance condition states that $R_0 R_d = 1$, which gives $e^{i2(\phi_0+\phi_d)} e^{i2k_x d} = 1$. The condition of waveguide modes can be rewritten as

$$k_x d + \phi_0 + \phi_d = m\pi, \quad m = 0, 1, 2 \ldots \tag{10}$$

When k_x is imaginary (corresponding to the surface modes), i.e., $k_x = ik_{xI}$, according to Eq. (9), parameters p and q are also imaginary: $p = ip_I$ and $q = iq_I$, where p_I and q_I are imaginary parts, defined as $p_I = -\varepsilon_V \alpha_1/(\varepsilon_1 k_{xI})$ and $q_I = -\varepsilon_g k_y/(\varepsilon_{xx} k_{xI})$. Hence the GH phase shifts are also imaginary, i.e., $2\phi_0 = i2\phi_{0I}^{(1)}$, $2\phi_d = i2\phi_{dI}^{(1)}$, where the imaginary parts can be given by

$$\phi_{0I}^{(1)} = -\tanh^{-1}(p_I - q_I), \tag{11}$$

$$\phi_{dI}^{(1)} = -\tanh^{-1}(p_I + q_I). \tag{12}$$

Eqs. (11) and (12) are used when $|p_I - q_I| \leq 1$ and $|p_I + q_I| \leq 1$. Furthermore, there is another solution for imaginary k_x when $|p_I - q_I| \geq 1$ and $|p_I + q_I| \geq 1$:

$$\phi_{0I}^{(2)} = -\tanh^{-1}\left[1/(p_I - q_I)\right], \tag{13}$$

$$\phi_{dI}^{(2)} = -\tanh^{-1}\left[1/(p_I + q_I)\right]. \tag{14}$$

For both of the solutions for imaginary k_x, according to $e^{-2[\phi_{0I}^{(n)} + \phi_{dI}^{(n)}]} e^{-2k_{xI}d} = 1$, the guidance condition can be rewritten as

$$k_{xI} d + \phi_{0I}^{(n)} + \phi_{dI}^{(n)} = 0, \quad n = 1, 2. \tag{15}$$

where the superscript $n = 1, 2$ denotes the two modes with imaginary k_x, corresponding to the surface magnetoplasmon polarition (SMP) modes. The first is an even mode in the absence of the external magnetic field, while the second is an odd one. In the presence of the applied magnetic field, since the magnetic fields in the gyrotropic medium become either cosh function or sinh function, to be shown in Eq. (17), hence we call the first mode as "cosh mode" and the second as "sinh mode".

For the symmetrical gyrotropic slab, according to the dispersion relations of the two media and guidance conditions, i.e., Eqs. (3), (4), and (10) or (15), we can get the numerical results for the magnetoplasma waves in the symmetrical slab. The results of dispersion relation in terms of dimensionless variables are illustrated in Fig. 2. The frequencies are normalized to the plasma frequency ω_p, and the wave numbers are normalized to k_p=ω_p/c. The material parameters used in the computation are: $\varepsilon_1 = \varepsilon_0$, $\varepsilon_\infty = 15.68\varepsilon_0$, $N = 2 \times 10^{22}\,\mathrm{m}^{-3}$, and $m^* = 0.014m_0 = 0.12753 \times 10^{-31}\,\mathrm{kg}$. Hence, $\omega_p = 1.7 \times 10^{13}\,\mathrm{rad/s}$ and $\omega_c/\omega_p = 0.737B_0$. These parameters correspond to an indium antimony (InSb) slab in free space.

When an external magnetic field is applied, there are two bands in the dispersion curve, as shown in Fig. 2. In the lower region, below the lower bulk solutions $k_x = 0$, there are two SMP modes (corresponding to cosh mode and sinh mode, shown in blue dashed lines and red dot lines), both of which start from the origin and rise just over the optical line which is plotted in dash-dot line. The cosh mode is continuous with the conventional waveguide mode (corresponding to the real k_x) of $m = 0$. Moreover, two higher waveguide modes corresponding to m=1 and 2 are also shown in Fig. 2. The waveguide modes are seen to become asymptotic to the frequency $\omega_H = \sqrt{\omega_c^2 + \omega_p^2}$ [31]. Similar phenomenon occurs in the upper frequency region except that there is no asymptotic frequency for the waveguide modes.

3. DISTRIBUTION OF THE FIELDS

In order to calculate the power flow in all media, we analyze the distribution of the fields in each region first. For TM waves, the magnetic fields for region 1 ($x < 0$), region 2 ($0 \le x \le d$), and region 3 ($x > d$) can be written as

$$\bar{H}_1(x, y) = \hat{z}H_1 e^{\alpha_1 x} e^{ik_y y}, \tag{16}$$

$$\bar{H}_2(x, y) = \begin{cases} \hat{z}H_1 \dfrac{\cos(k_x x + \phi_0)}{\cos\phi_0} e^{ik_y y} & \text{waveguide mode} \\ \hat{z}H_1 \dfrac{\cosh(k_{xI} x + \phi_{0I}^{(1)})}{\cosh\phi_{0I}^{(1)}} e^{ik_y y} & \text{cosh mode} \\ \hat{z}H_1 \dfrac{\sinh(k_{xI} x + \phi_{0I}^{(2)})}{\left|\sinh\phi_{0I}^{(2)}\right|} e^{ik_y y} & \text{sinh mode} \end{cases}, \tag{17}$$

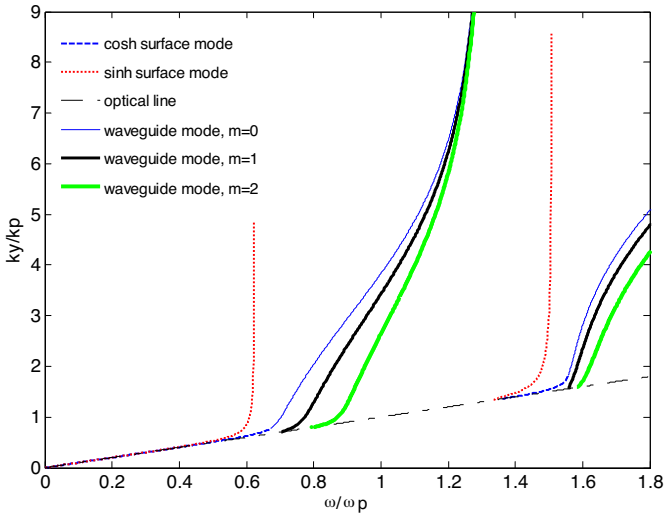

Figure 2. Dispersion in the symmetrical gyrotropic slab with the thickness of d in the Voigt configuration. The external magnetic field $B_0 = 1.2T$. The media are air-InSb-air, and the parameters are: $\varepsilon_1 = \varepsilon_0$, $\varepsilon_\infty = 15.68\varepsilon_0$, $\omega_p = 1.7 \times 10^{13}$ rad/s, $\omega_c/\omega_p = 0.737B_0$, and $d = 0.5\lambda_p = \pi c/\omega_p$.

$$\bar{H}_3(x,y) = \begin{cases} \hat{z}H_1 \dfrac{(-1)^m \cos\phi_d}{\cos\phi_0} e^{-\alpha_1(x-d)} e^{ik_y y} & \text{waveguide mode} \\ \hat{z}H_1 \dfrac{\cosh\phi_{dI}^{(1)}}{\cosh\phi_{0I}^{(1)}} e^{-\alpha_1(x-d)} e^{ik_y y} & \text{cosh mode} \\ \hat{z}H_1 \dfrac{-\sinh\phi_{dI}^{(2)}}{\left|\sinh\phi_{0I}^{(2)}\right|} e^{-\alpha_1(x-d)} e^{ik_y y} & \text{sinh mode} \end{cases} . \quad (18)$$

Taking a look at Eqs. (16), (17), and (18), one discovers that when an external magnetic field is applied, because of the difference of the two GH phase shifts at each boundary, $\left|\bar{H}_2(0,y)\right| \neq \left|\bar{H}_2(d,y)\right|$. It means that influenced by the external magnetic field, the distribution of the magnetic field is asymmetrical although the slab configuration is a symmetrical one.

The asymmetrical field distribution is more intuitively recognized by the inverted 'penetration' distance and effective guided thickness [32], as shown in Fig. 3. The effective guided thickness is not equal to the physical thickness because of the GH phase shifts. Detailed calculation [33, 34] reveals that the distances x_0 and x_d between the media interface and the effective interface can be approximately

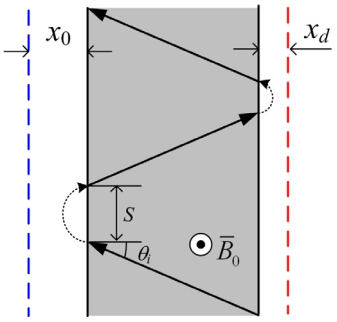

Figure 3. The effective guided thickness of the symmetrical gyrotropic slab. Because of the different GH phase shifts ϕ_0 and ϕ_d, the inverted 'penetration' distance x_0 is not equal to x_d, causing the distribution of the field to be asymmetrical.

expressed by

$$x_0 = -\frac{k_x}{2k_y}\frac{\partial 2\phi_0(k_y)}{\partial k_y}\bigg|_{k_y=k_{iy}} = \frac{1}{1+(p-q)^2}\left[\frac{p-q}{k_x} + \frac{k_x}{\alpha_1^2}p - \frac{k_x}{k_y^2}q\right], \quad (19)$$

$$x_d = -\frac{k_x}{2k_y}\frac{\partial 2\phi_d(k_y)}{\partial k_y}\bigg|_{k_y=k_{iy}} = \frac{1}{1+(p+q)^2}\left[\frac{p+q}{k_x} + \frac{k_x}{\alpha_1^2}p + \frac{k_x}{k_y^2}q\right]. \quad (20)$$

It is obvious to see that in the case of no external magnetic field, $q = 0$ and the GH phase shifts on both interfaces are the same, then the distance x_0 is equal to x_d, causing the center of the effective slab overlaps that of the physical one, therefore the field is symmetrically distributed in the slab. However, when there is an external magnetic field, q is no longer zero and the GH phase shifts on both sides are different, inducing the different extended distance x_0 and x_d. As a result, the center of the effective thickness shifts away from that of the physical one, causing the field asymmetrically distributed. We show the distribution of the magnetic field and the effective boundaries in Fig. 4. The center of the effective thickness and that of the magnetic field are close to each other.

As for the electric fields, it is easy to verify that, no matter which mode is concerned, the y components are all pure imaginary number, which results in the power flow only in the propagating direction, i.e., y direction. So we only consider the x components of electric fields in the three regions.

$$E_{1x}(x,y) = -\frac{k_y}{\omega\varepsilon_1}H_1 e^{\alpha_1 x}e^{ik_y y}, \quad (21)$$

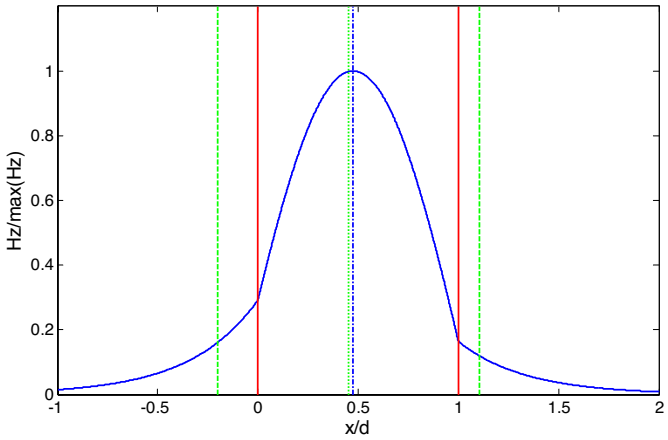

Figure 4. The distribution of magnetic field and the effective boundaries for the waveguide mode of $m = 0$. The vertical solid lines in red are the physical interfaces of the slab, while the dashed lines in green outside the slab are the effective guided boundaries. The center of the effective thickness (dash-dot line in green) and that of the magnetic field (dot line in blue) are shown in the slab. They are close to each other. The field is normalized to the maximum value, while the horizontal distances are normalized to the slab thickness d. The parameters are the same as those of Fig. 2 and the working frequency ω is 0.72 ω_p.

$$E_{2x}(x,y)=\begin{cases} -\frac{k_y}{\omega\varepsilon_V}H_1\frac{\cos(k_x x+\xi+\phi_0)}{\cos\phi_0\cos\xi}e^{ik_y y} & \text{waveguide mode} \\ -\frac{k_y}{\omega\varepsilon_V}H_1\frac{\sinh(k_{xI}x+\xi_I+\phi_{0I}^{(1)})}{\cosh\phi_{0I}^{(1)}|\sinh\xi_I|}e^{ik_y y} & \cosh\text{ mode} \\ -\frac{k_y}{\omega\varepsilon_V}H_1\frac{\cosh(k_{xI}x+\xi_I+\phi_{0I}^{(2)})}{\left|\sinh\phi_{0I}^{(2)}\right||\sinh\xi_I|}e^{ik_y y} & \sinh\text{ mode} \end{cases}, \quad (22)$$

here $\xi=\tan^{-1}\frac{\varepsilon_g k_x}{\varepsilon_{xx}k_y}$ and $\xi_I=\tanh^{-1}\frac{\varepsilon_{xx}k_y}{\varepsilon_g k_{xI}}$.

$$E_{3x}(x,y)=\begin{cases} -\frac{k_y}{\omega\varepsilon_1}H_1\frac{(-1)^m\cos\phi_d}{\cos\phi_0}e^{-\alpha_1(x-d)}e^{ik_y y} & \text{waveguide mode} \\ -\frac{k_y}{\omega\varepsilon_1}H_1\frac{\cosh\phi_{dI}^{(1)}}{\cosh\phi_{0I}^{(1)}}e^{-\alpha_1(x-d)}e^{ik_y y} & \cosh\text{ mode} \\ \frac{k_y}{\omega\varepsilon_1}H_1\frac{\sinh\phi_{dI}^{(2)}}{\left|\sinh\phi_{0I}^{(2)}\right|}e^{-\alpha_1(x-d)}e^{ik_y y} & \sinh\text{ mode} \end{cases}. \quad (23)$$

From Eqs. (17) and (22), we can find that compared with the

magnetic field in the gyrotropic medium, the x component of electric field has another phase shift ξ or ξ_I, also arisen from the applied magnetic field.

4. POYNTING VECTOR

In order to get deeper insight into the physics of guided waves, we proceed with calculation of energy flow in each medium. The time-averaged Poynting vectors in each region are

$$\left\langle \bar{S}_1 \right\rangle = \frac{1}{2}\mathrm{Re}\left(\bar{E}_1 \times \bar{H}_1^*\right) = \hat{y}\frac{k_y \left|H_1\right|^2}{2\omega\varepsilon_1}e^{2\alpha_1 x}, \tag{24}$$

$$\left\langle \bar{S}_2 \right\rangle = \frac{1}{2}\mathrm{Re}\left(\bar{E}_2 \times \bar{H}_2^*\right) = \begin{cases} \hat{y}\frac{k_y|H_1|^2}{4\omega\varepsilon_V \cos^2\phi_0}\left[\frac{\cos(2k_x x+2\phi_0+\xi)}{\cos\xi}+1\right] & \text{waveguide mode} \\ \hat{y}\frac{k_y|H_1|^2}{4\omega\varepsilon_V \cosh^2\phi_{0I}^{(1)}}\left[\frac{\sinh(2k_{xI}x+2\phi_{0I}^{(1)}+\xi_I)+\sinh\xi_I}{|\sinh\xi_I|}\right] & \cosh\text{ mode} \\ \hat{y}\frac{k_y|H_1|^2}{4\omega\varepsilon_V \sinh^2\phi_{0I}^{(2)}}\left[\frac{\sinh(2k_{xI}x+2\phi_{0I}^{(2)}+\xi_I)-\sinh\xi_I}{|\sinh\xi_I|}\right] & \sinh\text{ mode} \end{cases}, \tag{25}$$

$$\left\langle \bar{S}_3 \right\rangle = \frac{1}{2}\mathrm{Re}\left(\bar{E}_3 \times \bar{H}_3^*\right) = \begin{cases} \hat{y}\frac{k_y|H_1|^2}{2\omega\varepsilon_1}\frac{\cos^2\phi_d}{\cos^2\phi_0}e^{-2\alpha_1(x-d)} & \text{waveguide mode} \\ \hat{y}\frac{k_y|H_1|^2}{2\omega\varepsilon_1}\frac{\cosh^2\phi_{dI}^{(1)}}{\cosh^2\phi_{0I}^{(1)}}e^{-2\alpha_1(x-d)} & \cosh\text{ mode} \\ \hat{y}\frac{k_y|H_1|^2}{2\omega\varepsilon_1}\frac{\sinh^2\phi_{dI}^{(2)}}{\sinh^2\phi_{0I}^{(2)}}e^{-2\alpha_1(x-d)} & \sinh\text{ mode} \end{cases}. \tag{26}$$

From Eqs. (24), (25), and (26), we can see that in the isotropic media outside the waveguide, the time-averaged Poynting vector is always in the wave propagating direction, while it is not true for the gyrotropic medium in the slab. We show the spatial distribution of the time-averaged Poynting power and the corresponding magnetic and electric fields at a certain working frequency in Fig. 5. It is obvious to see that the y component of the Poynting power in the gyrotropic medium varies with the transverse position, and may be either positive or negative. This is because of the phase shift ξ or ξ_I between the

magnetic and electric fields, which directly comes from the ε_g, the influence of applied magnetic field. Hence this phenomenon cannot occur in the absence of the external magnetic field.

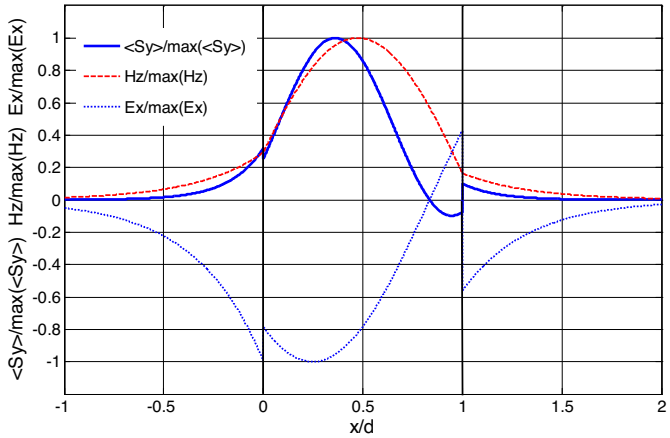

Figure 5. The spatial distribution of the time-average Poynting power in propagating direction, and corresponding magnetic and electric fields. Depending on the transverse position, $< S_y >$ in the gyrotropic medium may be either positive or negative while it is always positive in the isotropic media outside the slab. All the fields and the Poynting power are normalized to their maximum values respectively, while the horizontal distances are normalized to the slab thickness d. All the other parameters are the same as those of Fig. 4.

5. CONCLUSION

This paper investigates on the influence of an external magnetic field on a symmetrical gyrotropic slab in terms of GH phase shifts. Considering the nonreciprocity of the gyrotropic medium, we calculate the GH shifts on both sides of the symmetrical gyrotropic slab and derive the guidance conditions for both waveguide modes and surface modes. For TM waves, because of the different GH shifts at each boundary, the external magnetic field destroys the symmetry of spatial field distribution, the concepts of 'penetration' distance as well as effective thickness are used to illustrate the phenomenon. Moreover, the spatial distribution of the time-average Poynting power is also derived in terms of the GH phase shifts. It is found that influenced by the external magnetic field, the Poynting power along the waveguide direction in the slab varies with the transverse position, and may have positive or negative value simultaneously.

ACKNOWLEDGMENT

This work is sponsored by the Office of Naval Research under Contract N00014-06-1-0001, the Department of the Air Force under Air Force Contract F19628-00-C-0002, and the Chinese National Foundation under Contract 60531020.

REFERENCES

1. Kushwaha, M. S. and P. Halevi, "Magnetoplasmons in thin films in the Voigt configuration," *Phys. Rev. B*, Vol. 36, No. 11, 5960, 1987.
2. Kushwaha, M. S. and P. Halevi, "Magnetoplasmons in thin films in the perpendicular configuration," *Phys. Rev. B*, Vol. 38, No. 17, 12428, 1988.
3. Kushwaha, M. S. and P. Halevi, "Magnetoplasma modes in thin films in the Faraday configuration," *Phys. Rev. B*, Vol. 35, No. 8, 3879, 1987.
4. Gillies, J. R. and P. Hlawiczka, "TE and TM modes in gyrotropic waveguides," *J. Phys. D: Appl. Phys.*, Vol. 9, No. 9, 1315, 1976.
5. Gillies, J. R. and P. Hlawiczka, "Elliptically polarized modes in gyrotropic waveguides. II. An alternative treatment of the longitudinally magnetized case," *J. Phys. D: Appl. Phys.*, Vol. 10, 1891–1904, 1977.
6. Hlawiczka, P., "Elliptically polarized modes in gyrotropic waveguides," *J. Phys. D: Appl. Phys.*, Vol. 9, 1957–1965, 1976.
7. Hlawiczka, P., "A gyrotropic waveguide with dielectric boundaries: the longitudinally magnetised case," *J. Phys. D: Appl. Phys.*, Vol. 11, No. 8, 1157, 1978.
8. Hlawiczka, P., "The gyrotropic waveguide with a normal applied DC field," *J. Phys. D: Appl. Phys.*, Vol. 11, No. 14, 1941, 1978.
9. Eroglu, A. and J. K. Lee, "Dyadic Green's functions for an electrically gyrotropic medium," *Progress In Electromagnetics Research*, PIER 58, 223–241, 2006.
10. Li, L. W., N. H. Lim, and J. A. Kong, "Cylindrical vector wave function representation of Green's dyadic in gyrotropic bianisotropic media," *Journal of Electromagnetic Waves and Applications*, Vol. 17, No. 11, 1589–1591, 2003.
11. Li, L. W., N. H. Lim, W. Y. Yin, et al., "Eigenfunctional expansion of dyadic Green's functions in gyrotropic media using cylindrical vector wave functions - Abstract," *Journal of*

Electromagnetic Waves and Applications, Vol. 17, No. 12, 1731–1733, 2003.

12. Ivanov, S. T. and N. I. Nikolaev, "Magnetic-field effect on wave dispersion in a free semiconductor plasma slab," *J. Phys. D: Appl. Phys.*, Vol. 32, No. 4, 430, 1999.
13. Boardman, A., N. King, Y. Rapoport, et al., "Gyrotropic impact upon negatively refracting surfaces," *New J. Phys.*, Vol. 7, No. 1, 2005.
14. Eroglu, A. and J. K. Lee, "Wave propagation and dispersion characteristics for a nonreciprocal electrically gyrotropic medium," *Progress In Electromagnetics Research*, PIER 62, 237–260, 2006.
15. Zhang, M., L. W. Li, T. S. Yeo, et al., "Scattering by a gyrotropic bianisotropic cylinder of arbitrary cross section: an analysis using generalized multipole technique - Abstract," *Journal of Electromagnetic Waves and Applications*, Vol. 17, 1049–1051, 2003.
16. Yin, W. Y., L. W. Li, and M. S. Leong, "Scattering from multiple bianisotropic cylinders and their modeling of cylindrical objects of arbitrary cross-section - Abstract," *Journal of Electromagnetic Waves and Applications*, Vol. 14, 611–612, 2000.
17. Tan, E. L. and S. Y. Tan, "Cylindrical vector wave function representations of electromagnetic fields in gyrotropic bianisotropic media," *Journal of Electromagnetic Waves and Applications*, Vol. 13, 1461–1476, 1999.
18. Bass, F. and L. Resnick, "Spatial and temporal rotation of the polarization plane of electromagnetic waves reflected from and transmitted through a gyrotropic plate," *Journal of Electromagnetic Waves and Applications*, Vol. 17, 1131–1137, 2003.
19. Censor, D. and M. D. Fox, "Polarimetry in the presence of various external reflection and retrodirection mirroring mechanisms, for chiral and gyrotropic media," *Journal of Electromagnetic Waves and Applications*, Vol. 11, 297–313, 1997.
20. Huang, H., Y. Fan, B. Wu, et al., "Surface modes at the interfaces between isotropic media and uniaxial plasma," *Progress In Electromagnetics Research*, PIER 76, 1–14, 2007.
21. Kalluri, D. K., "Frequency shifting using magnetoplasma medium: Flash ionization," *IEEE T. Plasma. Sci.*, Vol. 21, No. 1, 77, 1993.
22. Talisa, S. H. and D. M. Bolle, "Performance predictions for isolators and differential phase shifters for the near-millimeter wave range," *IEEE T. Microw. Theory*, Vol. 29, No. 12, 1338,

1981.

23. Chen, Y. and B. Beker, "Analysis of bilateral coplanar waveguides printed on anisotropicsubstrates for use in monolithic MICs," *IEEE T. Microw. Theory*, Vol. 41, No. 9, 1489, 1993.
24. Kushwaha, M. S., "Effect of an applied magnetic field on interface excitations in finite layered structures. III," *Phys. Rev. B*, Vol. 40, No. 3, 1969, 1989.
25. Marques, R., F. L. Mesa, and M. Horno, "Nonreciprocal and reciprocal complex and backward waves in parallelplate waveguides loaded with a ferrite slab arbitrarily magnetized," *IEEE T. Microw. Theory*, Vol. 41, No. 8, 1409, 1993.
26. Zhang, M., T. S. Yeo, L. W. Li, et al., "Electromagnetic scattering by a multilayer gyrotropic bianisotropic circular cylinder - Abstract," *Journal of Electromagnetic Waves and Applications*, Vol. 17, 881–883, 2003.
27. Chung, S. K. and S. S. Kim, "An exact wave-optics analysis of optical wave-guide with anisotropic and gyrotropic materials," *J. Appl. Phys.*, Vol. 63, No. 12, 5654, 1988.
28. Prati, E., "Propagation in gyroelectromagnetic guiding systems," *Journal of Electromagnetic Waves and Applications*, Vol. 17, 1177–1196, 2003.
29. Lan, Y. C., Y. C. Chang, and P. H. Lee, "Manipulation of tunneling frequencies using magnetic fields for resonant tunneling effects of surface plasmons," *Appl. Phys. Lett.*, Vol. 90, No. 17, 2007.
30. Sarid, D., "Enhanced magnetic interaction of surface-magnetoplasmon polaritons," *IEEE J. Quantum Elect.*, Vol. 20, No. 8, 943–948, 1984.
31. Kushwaha, M. S., "Plasmons and magnetoplasmons in semiconductor heterostructures," *Surf. Sci. Rep.*, Vol. 41, No. 1–8, 5, 2001.
32. Tsakmakidis, K. L., A. D. Boardman, and O. Hess, "'Trapped rainbow' storage of light in metamaterials," *Nature*, Vol. 450, No. 7168, 397, 2007.
33. Brekhovskikh, L. M., *Waves in Layered Media*, 2nd edition, Academic, New York, 1980.
34. Chen, J. J., T. M. Grzegorczyk, B. I. Wu, et al., "Role of evanescent waves in the positive and negative Goos-Hänchen shifts with left-handed material slabs," *J. Appl. Phys.*, Vol. 98, No. 094905, 2005.